THE IMPORTANCE OF ACCURATE COMPUTATION OF SECONDARY ELECTRON EMISSION FOR MODELING SPACECRAFT CHARGING

S. Clerc,
Alcatel Space, 100 boulevard du Midi, Cannes la Bocca, FRANCE,
tel / fax: +33(0) 492 926 052 / 970, Sebastien.Clerc@space.alcatel.fr

J.R. Dennison, C.D. Thomson,
Physics Department UMC 4415
Utah State University
Logan, UT 84322-4415

Office: (435)797-2936
Lab: (435) 797-0925

Abstract

Secondary electron emission is a critical contributor to the current balance in spacecraft charging. Spacecraft charging codes use a parameterized expression for the secondary electron yield $\delta(E_o)$ as a function of incident electron energy E_o. Simple three-step physics models of the electron penetration, transport and emission from a solid are typically expressed in terms of the incident electron penetration depth at normal incidence or range $R(E_o)$, and the mean free path of the secondary electron, $\lambda(E)$. We recall classical models for the range R(Eo): a power law expression of the form $b_1E_o^{n1}$, and a more general empirical bi-exponential expression $R(E_o) = b_1E_o^{n1}+b_2E_o^{n2}$. Expressions are developed that relate the theoretical fitting parameters (λ, b_1, b_2, n_1 and n_2) to experimental terms (the energy E_{max} at the maximum secondary electron yield δ_{max}, the first and second crossover energies E_1 and E_2, and the asymptotic limits for $\delta(Eo \rightarrow \infty)$). In most models, the yield is the result of an integral along the path length of incident electrons. Special care must be taken when computing this integral. An improved fourth-order numerical method is presented and compared to the standard second-order method. A critical step in accurately characterizing a particular spacecraft material is the determination of the model parameters in terms of the measured electron yield data. The fitting procedures and range models are applied to several measured data sets to compare their effectiveness in modeling the function $\delta(Eo)$ over the full range of incident energies, and in particular for determining crossover energies and critical temperatures.

Introduction

Secondary electron emission (SEE) is an important contributer in the current balance driving spacecraft charging. Most spacecraft surfaces are generally covered with low yield materials (Kapton®, metals, graphite) which leads to large negative absolute potential. On the other hand, some dielectric materials such as glass have a high secondary emission yield and build up large positive surface charging. This results in the much dreaded inverse gradient situation, a major source of electrostatic discharges. Another important aspect of secondary emission is its strong variation with the incident energy, which leads to threshold effects (see [1]). As noted in [2], an accurate modeling of SEE is therefore crucial to the simulation of spacecraft charging. It is particularly important to get the correct behavior at high incident energy, since the flux of magnetosphere electrons is peaked at some tens of keV.

Measuring SEE properties of materials is particularly difficult task [3]. It is especially true for dielectric materials, because the implanted charges and the resulting internal electric field modify the trajectories of the incident and secondary electrons [4]. This point is however outside the scope of the present study.

Modeling SEE is also a difficult point. Although all the models of the literature correctly predict a SEE maximum around 100-700 eV, they differ greatly at high incident energy. A first source of difference is the way the incident electron penetration inside the material is modeled. In this work, we concentrate on range models using a power-law or a sum of two power-laws. The models may then differ in the way they account for the creation and propagation of secondary electrons. We concentrate here on a three-step model with an exponential escape potential. We will show that even with a specified model, computational issues and fitting strategies can also lead to significant differences in the predictions.

THE THREE STEP MODEL

The amount of secondary electrons created at a given point of the trajectory of the incident electron is proportional to the loss of kinetic energy $dE/dx = S(x)$. Among these secondary electrons, a fraction will actually escape to the surface and contribute to the secondary emission current. This dependency is modeled through an escape potential $f(x)$, which is a decreasing function of the depth x.

The contribution of all secondary electrons is integrated along the particle path to get the total secondary emission yield:

$$\delta(E_0) = \int_0^{R(E_0)} S(E_0, x) f(x) dx \tag{1}$$

It is reasonable to assume that the escape potential f decays exponentially with the depth:

$$f(x) = A e^{-x/\lambda} \tag{2}$$

The parameters A and λ are material-dependent. They are not measured directly, so they have to be determined from the properties of the SEE yield.

Here S is the stopping power of the particle with incident energy E_0 at point x, and f is a positive decreasing function. The integral extends to the end of the trajectory, which is given by the range $R(E_0)$. If E is the remaining kinetic energy of an electron of incident energy E_0 at a depth x, then

$$x = R(E_0) - R(E) \tag{3}$$

holds. This is the so-called Continuous Slowing Down Approximation (CSDA). The stopping power is the energy decay rate

$$S(x) = -\frac{dE}{dx}.$$

Using (3), the stopping power can be related to the range:

$$S(E) = \frac{1}{R'(E)} \tag{4}$$

RANGE MODEL

At high energy, the range behaves like a power law E^n with $n > 1$. For a better fit at incident energy below 1 keV, a bi-exponential function $R(E) = b_1 E^{n_1} + b_2 E^{n_2}$ with $n_1 < 1$ has been introduced (ref [5]). The range has an inflection point for some incident energy E_{Bragg} which corresponds to a maximum for the stopping power known as the Bragg peak. A plot of the typical stopping power S(x) as a function of the path length is shown in Figure 1 . Most of the energy of the incident electron is released around the Bragg peak, close to the end of the trajectory.

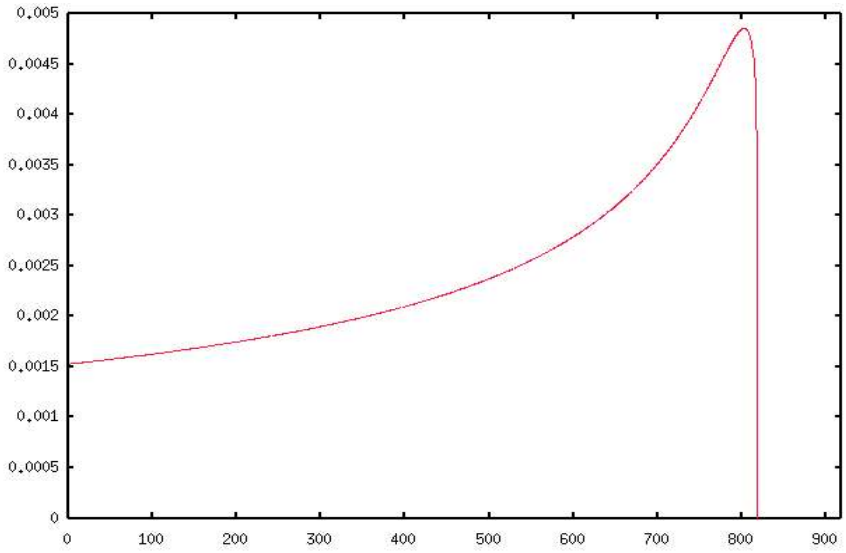

Figure 1: The Bragg curve (stopping power as a function of the path length).

High energy asymptotics

Using (3), we perform a change of variable in equation (1):

$$\delta(E_0)=\int_0^{E_0} f\left(R(E_0)-R(E)\right)dE. \tag{5}$$

Differencing equation (5), we find that δ satisfies the following fundamental differential equation:

$$\frac{d\,\delta}{dE}=A-R'(E)\,\delta/\lambda \tag{6}$$

From this equation we will derive some useful properties of the yield function. It is also a convenient form for numerical computations (see below).

Applying equation (6) at the energy E_{max} of the maximum yield gives an interesting relation between A and λ

$$A=\delta_{max}\,R'(E_{max})/\lambda\,. \tag{7}$$

At high energy both δ and δ' tend to zero. In view of equation (6) we have:

$$\lim_{E\to\infty}\delta=\frac{\lambda\,A}{R'(E)}=\delta_{max}\frac{R'(E_{max})}{R'(E)}=\delta_{max}\frac{S(E)}{S(E_{max})} \tag{8}$$

Asymptotically, the secondary yield is thus proportional to the stopping power, with a coefficient which depends only on the value at maximum yield.

Numerical computation

Computing an approximation of integral (1) is a difficult task, similar to that of computing special functions. Its requires high order approximation methods. Moreover as S(x) is known only implicitly, usual quadrature formulas are not practical.

Several authors use a very crude 1st order approximation, replacing S(x) by its value S(0) at the surface. The integral is thus approximated by

$$\delta \approx A\lambda \frac{(1-e^{-R(E)/\lambda})}{R'(E)} \quad .$$

NASCAP [5] uses a 2nd order approximation based on a linearization of S(x) at x = 0. In view of figure 1, it is clear that a linear approximation of S(x) will not reproduce the Bragg peak, and therefore underestimate the total stopping power. Secondary electrons created near the Bragg peak will not be taken into account if it occurs far from the surface. The impact on the computed SEE yield will depend on the value of λ. If it is large then the secondary electrons created relatively deeply inside the material will be able to reach the surface, so the approximation error will be significant.

Looking at figure 1 again, it is clear that only a 4th order approximation will be able to reproduce the shape of the stopping power curve S(x). However, a fourth order expansion at x = 0 would be cumbersome. Instead, we suggest to integrate equation (6) between E = 0 and E = E_0 by a fourth order Backward Differencing Formula (with four intermediate steps).

TWO STRATEGIES TO DETERMINE THE MODEL PARAMETERS

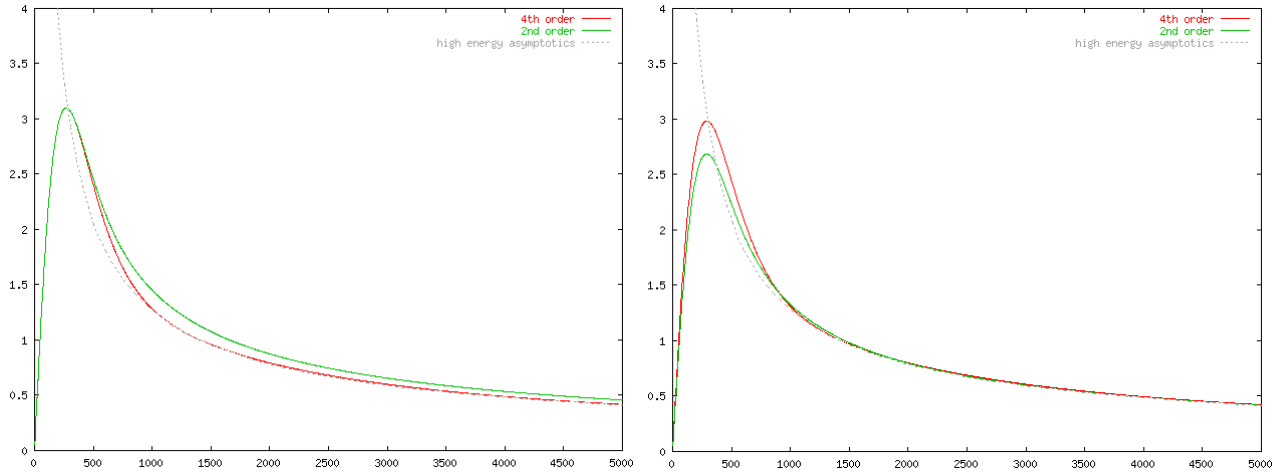

Figure 2: three-step model for SEE, computed with a 2nd order (green) or 4th order (red) method. Left: maximum fitting strategy. Right: asymptotic fitting. Dashed line : high energy asymptotics (8).

The three-step model involves two free parameters A and λ. These parameters can however not be measured directly, and must be related to SEE yield values. A first strategy consists in using the energy and value of the maximum SEE yield δ_{max} and E_{max}. This is the maximum-fitting strategy.

An alternate strategy consists in solving for λ such that $\delta'(E_{max}) = 0$ with A given by equation (7). This asymptotic-fitting strategy ensures that the correct behavior at infinity (equation 8) is satisfied.

In figure 2 we have compared the two strategies combined with either a 2nd order or 4th order method for given values of δ_{max} and E_{max} and a given power-law for the range model. With the maximum-fitting strategy, only the 4th order approximation satisfies the asymptotics of equation (8). A direct consequence is the difference in the predicted second crossover energy. This energy E_2 defined by $\delta(E_2) = 1$ is 1410 eV for the 4th order method and 1740 eV for the 2nd order method. The relative error is 15 %.

With the asymptotic-fitting strategy, the actual maximum yield obtained with the 2nd order method is off its real value by 10 %. With the 4th order method, the computed maximum is very close to the actual value. Note that in this case the computed values of parameters A and λ are similar with the two methods. The difference in the second crossover energy between the two methods is now smaller than 3%.

CRITICAL TEMPERATURE

As an illustration, we compute the critical temperature for several materials using either the 2nd order or the 4th order approximation. The critical temperature for a Maxwellian plasma environment is the temperature above which charging

occurs, i.e. the temperature such that the total secondary electron emission current balances exactly the incident current (see e.g. [1][6][2]). For a Maxwellian plasma with temperature T, the average yield is:

$$\begin{aligned}\langle\delta\rangle(kT) &= \frac{1}{2\,\pi(kT)^2}\int_0^\infty\int_0^{\pi/2}\int_0^{2\pi}(v\cos\theta)\,f(v)\,\delta(v,\theta)\,v^2\sin\theta\,d\theta\,d\phi\,dv \\ &= \frac{1}{2\,(kT)^2}\int_0^\infty\int_0^{\pi/2} E\,f(E)\,\delta(E,\theta)\cos\theta\sin\theta\,d\theta\,dE \\ &= \frac{1}{2}\int_0^\infty\int_0^{\pi/2} x\,e^{-x}\,\delta(x\,kT,\theta)\cos\theta\sin\theta\,d\theta\,dx\end{aligned}$$

The critical temperature T_c is defined by the equation $\langle\delta\rangle(kT_c)=1$.

In table 1 we have listed numerical results for three materials, using either the 2nd or the 4th order method with both fitting strategies. We have chosen high-yield materials for which the difference is particularly significant. One can see that the 2nd order method used with the maximum-fitting strategy introduces a large error (20 %). With the asymptotic-fit strategy the error is reduced to below 3 %. With the 4th order method, the two fitting strategies give similar results.

Material	δ_{max}	E_{max} ***(eV)***	***Range***	***2nd order (asymptotic fit)***	***2nd order (max fit)***	***4th order (asymptotic fit)***	***4th order (max fit)***
TEFLON®	3	300	$45.4\,E^{0.4}+218\;E^{1.77}$	3.9	4.9	4.1	4.1
Cover glass	5.8	1000	$77.5\,E^{0.45}+156\;E^{1.73}$	35.5	44	36.7	36.8
Anodized aluminum	3.05	290	$E^{1.7}$	3.7	4.5	3.8	3.8

Table 1: Critical temperature (in keV) for some materials.

FITTING STRATEGY FOR EXPERIMENTAL DATA

Fitting the model parameters to experimental data also depends on the method used to compute the integral (1). If a low order method is used, a maximum-fitting strategy and an asymptotic-fitting strategy may give different results.

An asymptotic-fitting strategy to determine optimal model parameters was used in [7]. Parameters A and λ are determined to get the correct behavior at high energy. If the escape length λ of the material is large, this may result in a wrong value for the maximum yield δ_{max}. However, as advocated above, this strategy is preferable in the context of spacecraft charging applications.

With the 4th order method, it is generally possible to fit both the maximum value and the asymptotic behavior.

This point is detailed in the following sections.

Conductors

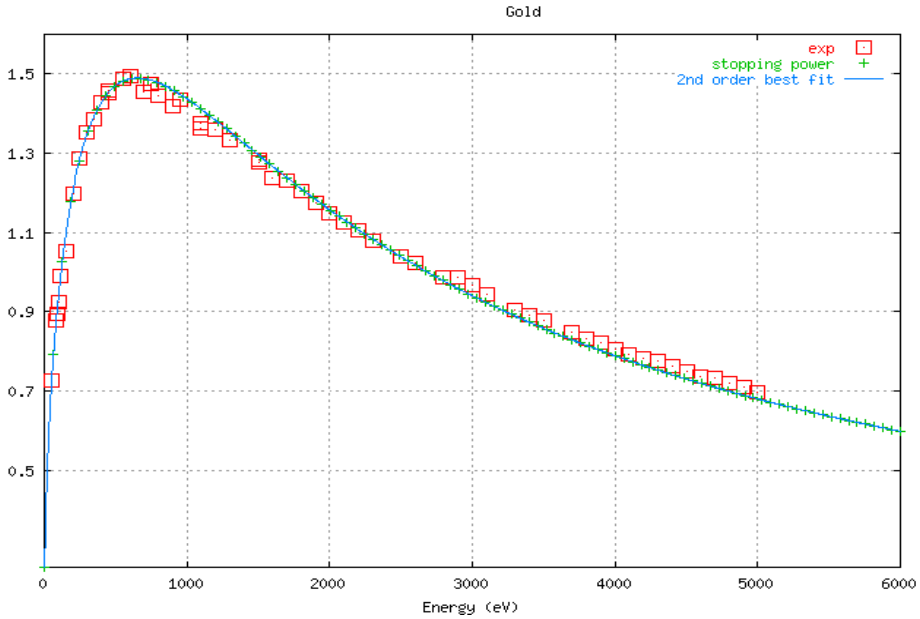

Figure 3: Fit to experimental points for gold.

In conductors the escape length is usually small. Most of the emitted secondary electrons are created close to the surface. The escape potential is close to a Dirac mass and the integral (1) can be replaced by the asymptotic expansion (8). The order of approximation in the integral is therefore irrelevant.

It is possible to adjust the coefficients of the bi-exponential range model to fit experimental points. For homogeneity reasons and because E_{max} has to satisfy $R''(E_{max}) = 0$, there are only two free parameters: $n_1 < 1$ and $n_2 > 1$ which account respectively for the behavior at low energy and high energy. These coefficients may be determined as the slopes of the asymptotes in a log-log graph.

Dielectrics

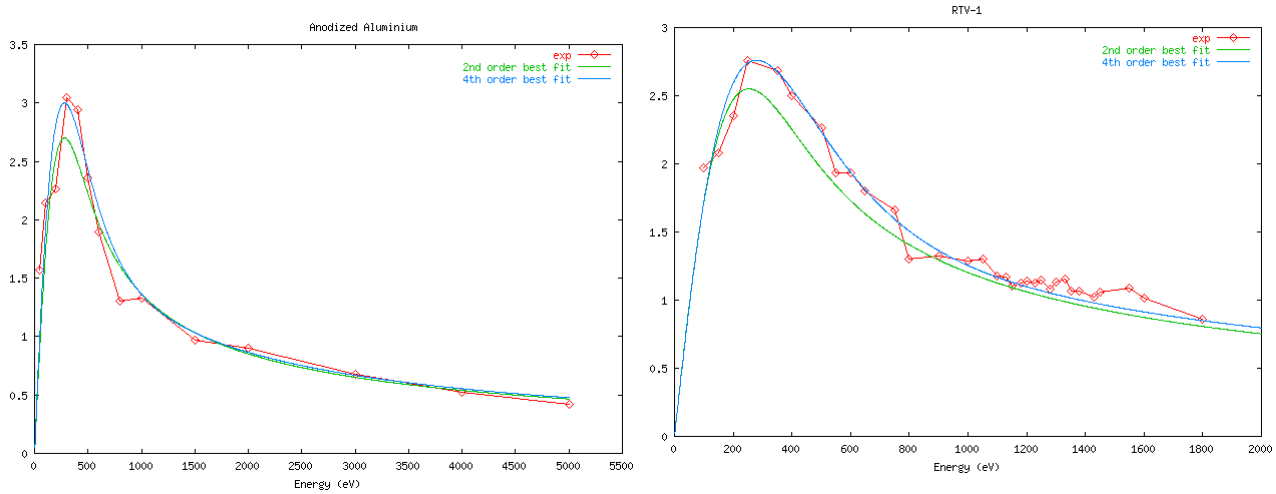

Figure 4: Fit to experimental SEE yield for anodized aluminum (left) and RTV adhesive (right).

For dielectrics, the escape length is generally larger. The integral (1) has to be computed precisely. On the other hand, it is generally enough to use a simple power law for the range model. This power can be determined again as the slope of

the high energy asymptote of the SEE yield in the log-log graph.

On the other hand, if the integral is not computed with enough precision, it is not possible to recover the correct high energy asymptotics unless by lowering the maximum yield δ_{max}. This situation is shown for two high-yield dielectric materials (anodized aluminum and RTV-silicone adhesive NuSil CV-1147) in figure 4. The best fit with the 2nd order accurate method can not be arranged to reach the maximum yield, whereas the 4th order accurate method is significantly closer to experimental points.

Conclusion

The three-step model is widely used for the computation of SEE yield of materials. The numerical computation of this model has to been done carefully if one wants to recover the correct behavior at high energy. A 4th order approximation has been show to give more accurate results than usual low-order approximations. If a low-order approximation is used nevertheless, a fitting strategy which concentrates on the high-energy asymptote rather than the maximum yield is advised.

References

[1]: **Laframboise J.G., Kamitsuma M., Godard R.**, "Multiple floating potentials, 'Threshold-Temperature' effects and 'Barrier'", *Int. Symp. on Spacecraft Materials in Space Env.*, Toulouse (France), 1982

[2]: **Katz I., Mandell M., Jongeward G.**, The importance of accurate secondary electron yields in modeling spacecraft, *J. of Geophysical Research*, 1986

[3]: **Dennison J.R., Thomson C.D., Kite J., Zavyalov V., Corbridge J.**, "Materials Characterization at Utah State University", *8th Int. Conf. on Solid Dielectrics*, Toulouse (France), 2004

[4]: **Davies R.E., Dennison J.R.**, "Evolution of Secondary Electron Emission Characteristic of S/C Surfaces", *6th Spacecraft Charging Technology Conference*, Hanscom (USA), 1998

[5]: **Mandell M.J., Stannard P.R., Katz I.**, *NASCAP programmer's reference manual*, 1984

[6]: **Lai S.T.**, Spacecraft charging threshold in single and double Maxwellian space environ, *IEEE Trans. Nucl. Sci.*, 1991

[7]: **Thomson C.D.**, *Measurements of the secondary electron emission properties of insulators*, PhD thesis, Utah State U., 2005